



NIH Public Access

Author Manuscript

Inorg Chem. Author manuscript; available in PMC 2007 January 10.

Published in final edited form as:
Inorg Chem. 2004 May 3; 43(9): 2932–2942.

Variable π -Bonding in Iron(II) Porphyrinates with Nitrite, CO and *tert*-Butyl Isocyanide. Characterization of $[\text{Fe}(\text{TpiVPP})(\text{NO}_2)(\text{CO})]^-$

Habib Nasri[†], Mary K. Ellison[‡], Maoyu Shang[‡], Charles E. Schulz[§], and W. Robert Scheidt[‡]

[†] Faculté des Sciences de Monastir

[‡] University of Notre Dame

[§] Knox College

Abstract

The addition of the strongly π -bonding ligands CO or *tert*-butyl isocyanide to the low-spin five-coordinate iron(II) nitrite species, $[\text{Fe}(\text{TpiVPP})(\text{NO}_2)]^-$, (TpiVPP = picket fence porphyrin) gives two new six-coordinate species $[\text{Fe}(\text{TpiVPP})(\text{NO}_2)(\text{CO})]^-$ and $[\text{Fe}(\text{TpiVPP})(\text{NO}_2)(t\text{-BuNC})]^-$. These species have been characterized by single-crystal structure determinations and by UV-vis, IR and Mössbauer spectroscopies. All evidence shows that in the mixed-ligand iron(II) porphyrin species, $[\text{Fe}(\text{TpiVPP})(\text{NO}_2)(\text{CO})]^-$, the two trans, π -accepting ligands CO and nitrite compete for π density. The CO ligand however dominates the bonding. The Fe–N(NO_2) bond lengths for the two independent anions in the unit cell at 2.006(4) and 2.009(4) Å are lengthened compared to other nitrite species with either no trans ligands or non- π -accepting trans ligands to nitrite. The Fe–C(CO) bond lengths are 1.782(4) Å and 1.789(5) Å for the two anions. The two Fe–C–O angles at 175.5(4)° and 177.5(4)° are essentially linear in both anions. The quadrupole splitting for $[\text{Fe}(\text{TpiVPP})(\text{NO}_2)(\text{CO})]^-$ was determined to be 0.32 mm/s and the isomer shift was 0.18 mm/s at room temperature in zero applied field. Both of the Mössbauer parameters are much smaller than those found for six-coordinate low-spin iron(II) porphyrinates with neutral nitrogen-donating ligands as well as iron(II) nitro complexes. However, the Mössbauer parameters are typical of other six-coordinate CO porphyrinates signifying that CO is the more dominant ligand. The CO stretching frequency of 1974 cm⁻¹ is shifted only slightly to higher energy compared to six-coordinate CO complexes with neutral nitrogen-donor ligands trans to CO. Crystal data for $[\text{K}(222)][\text{Fe}(\text{TpiVPP})(\text{NO}_2)]^-(\text{CO}) \cdot 1/2\text{C}_6\text{H}_5\text{Cl}$: monoclinic, space group $P2_1/c$, $Z = 8$, $a = 33.548(6)$ Å, $b = 18.8172(15)$ Å, $c = 27.187(2)$ Å, $\beta = 95.240(7)$ °, $V = 17091(4)$ Å³.

Introduction

The binding of the diatomic molecules O₂, CO, and NO to heme proteins is extremely important to mammalian physiology, while the binding of nitric oxide (NO), nitrite (NO₂⁻) and nitrate (NO₃⁻) to hemes is involved in important denitrification processes. Hence, the study of the bonding interaction between these biologically significant small molecules and others to hemes has been and continues to be an active area of research.^{1–3} However, despite great advances in understanding the many biological functions of these molecules, there remains considerable

Correspondence to: Charles E. Schulz; W. Robert Scheidt.

Contribution from The Department of Chemistry and Biochemistry, University of Notre Dame, Notre Dame, Indiana 46556, Faculté des Sciences de Monastir, Avenue de l'environnement, 5019 Monastir, Tunisia and Department of Physics, Knox College, Galesburg, Illinois 61401

Supporting Information Available: Tables S1–S6, giving complete crystallographic details, atomic coordinates, bond distances and angles, anisotropic temperature factors, and fixed hydrogen atom positions for $[\text{K}(222)][\text{Fe}(\text{TpiVPP})(\text{NO}_2)(\text{CO})] \cdot 1/2\text{C}_6\text{H}_5\text{Cl}$ and Figures of K(222) cations and complete labelled diagrams of the $[\text{Fe}(\text{TpiVPP})(\text{NO}_2)(\text{CO})]^-$ anions. (PDF). An X-ray crystallographic file, in CIF format, is available. This material is available free of charge via the Internet at <http://pubs.acs.org>.

controversy about the mechanisms and identities of possible intermediates involved in their numerous reactions. For instance, the discrimination in binding of O₂ over CO to hemes in respiration is not completely understood.^{4, 5} In addition, it is proposed that many of the intermediates in the inorganic nitrogen cycle involve the interaction of hemes with small nitrogen containing molecules; the exact identities of several are only speculative. In a recent mechanistic study⁶ of the reduction of nitrite to ammonia by cytochrome c nitrite reductase (ccNiR) it was proposed that the binding of nitrite to an iron(II) heme which starts the reaction cycle depends on the strong *pi* bond between nitrite and iron(II). The π bond leads to a strong Fe–N bond and a weakened N–O bond which can be cleaved heterolytically. Hence, the nature of the bond between nitrite and iron is critically important to the activation of this enzyme. Clearly, gaining insight into the bonding interaction between these small molecules and hemes through structural and physical studies is of interest.

Experimental Section

General Information

All manipulations for the preparation of the iron(II) six-coordinate porphyrin derivatives (see below), were carried out under argon using a double-manifold vacuum line, Schlenkware and cannula techniques. Chlorobenzene was purified by washing with concentrated sulfuric acid, then with water until the aqueous layer was neutral, then dried with MgSO₄, and then distilled twice over P₂O₅.²⁹ Hexanes were distilled from sodium/benzophenone. KNO₂ was recrystallized twice from hot distilled water, dried overnight at about 75°C and stored under argon. Kryptofix-222 (Aldrich) was recrystallized from benzene (distilled from sodium/benzophenone) and stored under argon in the dark. The free base, (H₂TpivPP), and the corresponding iron(III) chloro and triflato derivatives were synthesized by literature methods.^{30,31} UV-vis spectra were recorded on a Perkin-Elmer Lambda 19 UV/vis/near-IR spectrometer and IR spectra were recorded on a Perkin-Elmer Paragon 10000 FT-IR spectrometer as KBr pellets. Mössbauer measurements were performed on a constant acceleration spectrometer from 4.2 K to 300 K with optional small field and in a 9 T superconducting magnet system (Knox College). A sample of [K(222)][Fe(TpivPP)(NO₂)(CO)]·1/2C₆H₅Cl for Mössbauer spectroscopy was prepared by immobilization of the crystalline material (crystals not ground but washed with water under argon) in Apiezon M grease.

Synthesis of [K(222)][Fe(TpivPP)(NO₂)(CO)]·1/2C₆H₅Cl

[Fe(TpivPP)(SO₃CF₃)·(H₂O)] (20 mg, 0.016 mmol) and ~1 mL of zinc amalgam in 8 mL of chlorobenzene were stirred for about 1 hour under argon. The deep red solution of [Fe(TpivPP)] was filtered into a second solution prepared by stirring (overnight) 80 mg of Kryptofix-222 (0.2 mmol) and 185 mg of KNO₂ (2.2 mmol) in 7 mL of chlorobenzene. A stream of CO gas was passed (for about 15 min) through the dark red-yellow solution of the five-coordinate (nitro)iron(II) species, [Fe(TpivPP)(NO₂)]⁻.²⁰ The color changes slightly to light red as a result of forming the six-coordinate product [Fe(TpivPP)(NO₂)(CO)]⁻. Single crystals of this complex were prepared by slow diffusion of hexanes into the chlorobenzene solution. UV-vis in C₆H₅Cl: λ_{max} , nm (log ε): 414 (sh) (4.67); 434 (5.30); 546 (3.98). IR (KBr): v(CO) 1974 (m) cm⁻¹; v(NO₂) 1383

Results

Reaction of the five-coordinate iron(II) species, [Fe(TpivPP)(NO₂)]⁻, with CO or *tert*-butyl isocyanide gives the new anionic, six-coordinate iron(II) complexes [Fe(TpivPP)(NO₂)(CO)]⁻ and [Fe(TpivPP)(NO₂)(*t*-BuNC)]⁻. Care must be taken to eliminate halide impurities that are known to coordinate strongly to iron(II) species. Hence, chlorobenzene was washed with concentrated sulfuric acid and Kryptofix-222 and KNO₂ were recrystallized. The two six-

coordinate species were characterized in solution with UV-visible spectroscopy using a specialized inert-atmosphere cell with 1 and 10-mm path lengths. Crystalline anionic iron porphyrinates were obtained as potassium-(Kryptofix-222) salts. Both species were characterized by infrared spectroscopy. The carbonyl stretching frequency for $[\text{Fe}(\text{TpiVPP})(\text{NO}_2)(\text{CO})]^-$ appears at 1974 cm^{-1} . The C–N stretch is at 2101 cm^{-1} for $[\text{Fe}(\text{TpiVPP})(\text{NO}_2)(t\text{-BuNC})]^-$. The solid-state Mössbauer quadrupole splitting, ΔE_Q , for $[\text{K}(222)][\text{Fe}(\text{TpiVPP})(\text{NO}_2)(\text{CO})] \cdot 1/2\text{C}_6\text{H}_5\text{Cl}$ was found to be 0.32 mm/s and the isomer shift, δ , was 0.18 mm/s at room temperature in zero applied field.

Discussion

Over the past several years, we have synthesized a number of (nitro)iron(II) porphyrin species. The successful syntheses of these complexes results from the strategic use of picket fence porphyrin and cryptate (or macrocyclic crown ether) cations. The five-coordinate anionic iron (II) nitrite species, $[\text{Fe}(\text{TpiVPP})(\text{NO}_2)]^-$, is prepared by addition of cryptand-solubilized KNO_2 to the highly air-sensitive four-coordinate species $[\text{Fe}(\text{TpiVPP})]$. All of the characterized six-coordinate (nitro)iron(II) species result from the anaerobic addition of gaseous NO or CO or by addition of excess neutral ligand such as pyridine, pentamethylene sulfide, or *t*-butyl isocyanide to $[\text{Fe}(\text{TpiVPP})(\text{NO}_2)]^-$ in solution. As shown by electronic spectroscopy, all of these six-coordinate species persist in solution under anaerobic conditions. In fact, the spectroscopic characterization of $[\text{Fe}(\text{TpiVPP})(\text{NO}_2)]^-$ and the resulting six-coordinate species $[\text{Fe}(\text{TpiVPP})(\text{NO}_2)(\text{L})]^-$ was our first indication that nitrite is a very unusual ligand. We begin our discussion with the effects of the ligands NO_2^- and CO on the electronic spectrum.

The electronic spectrum of $[\text{Fe}(\text{TpiVPP})(\text{NO}_2)]^-$ has a Soret band at 444 nm . As can be seen from the electronic spectral data summarized in Table 2, this 444 nm Soret band for low-spin five-coordinate $[\text{Fe}(\text{TpiVPP})(\text{NO}_2)]^-$ is strongly red-shifted compared to all of the other five- or six-coordinate iron(nitro) species thus far characterized. It is also strongly red-shifted compared to the spectrum of five-coordinate $[\text{Fe}(\text{TPP})(\text{CO})]$. The addition of a neutral ligand such as PMS or pyridine to $[\text{Fe}(\text{TpiVPP})(\text{NO}_2)]^-$ causes the Soret band to blue shift by more than 10 nm . A similar blue shift in the Soret occurs upon addition of NO to the five-coordinate nitrite species. The Soret band at 407 nm for the low-spin, five-coordinate species $[\text{Fe}(\text{TpiVPP})(\text{NO})]$ is very blue shifted compared to $[\text{Fe}(\text{TpiVPP})(\text{NO}_2)]^-$. So what shift in the position of the Soret band should one expect when CO is added trans to nitrite? Probably the most well-known porphyrin CO-related spectroscopic change occurs when CO is added to five-coordinate high-spin thiolate hemes. These are the P450-type porphyrin derivatives, so-called because of the intense red-shifted Soret band at $\sim 450 \text{ nm}$. A small red shift is also seen when a CO ligand is added to the five-coordinate $[\text{Fe}(\text{TPP})(\text{CO})]$ species to give $[\text{Fe}(\text{TPP})(\text{CO})_2]$.

The average equatorial $\text{Fe}-\text{N}_\text{p}$ bond length for $[\text{Fe}(\text{TpiVPP})(\text{NO}_2)(\text{CO})]^-$ (**1**) is $1.992(7) \text{ \AA}$ and for $[\text{Fe}(\text{TpiVPP})(\text{NO}_2)(\text{CO})]^-$ (**2**) is $1.997(6) \text{ \AA}$. These average bond lengths are the same as those found for the six-coordinate nitro species $[\text{Fe}(\text{TpiVPP})(\text{NO}_2)(\text{PMS})]^-$,²² $[\text{Fe}(\text{TpiVPP})(\text{NO}_2)(\text{Py})]^-$,²² and $[\text{Fe}(\text{TpiVPP})(\text{NO}_2)(\text{NO})]^-$.²¹ The average distance for these six-coordinate species is 0.02 \AA longer than in the five-coordinate nitro species, $[\text{Fe}(\text{TpiVPP})(\text{NO}_2)]^-$. It is also slightly shorter (by 0.01 \AA) than the $\text{Fe}-\text{N}_\text{p}$ bond length average of other CO complexes (confer Table 3).

The iron–axial ligand bond lengths are sensitive to bonding changes and the largest structural changes occur upon coordination of a sixth ligand. The $\text{Fe}-\text{N}(\text{NO}_2)$ bond lengths for $[\text{Fe}(\text{TpiVPP})(\text{NO}_2)(\text{CO})]^-$ (**1**) and $[\text{Fe}(\text{TpiVPP})(\text{NO}_2)(\text{CO})]^-$ (**2**) are $2.006(4) \text{ \AA}$ and $2.009(4) \text{ \AA}$, respectively. These are 0.16 \AA longer than the $\text{Fe}-\text{N}(\text{NO}_2)$ bond length

Supplementary Material

Refer to Web version on PubMed Central for supplementary material.

Acknowledgements

We thank the National Institutes of Health for support of this research under Grant GM-38401. Funds for the purchase of the FAST area detector diffractometer were provided through NIH Grant RR-06709 to the University of Notre Dame.

References

1. Wyllie GRA, Scheidt WR. Chem Rev 2002;102:1067. [PubMed: 11942787]
2. Averill BA. Chem Rev 1996;96:2951. [PubMed: 11848847]
3. Scheidt WR, Ellison MK. Acc Chem Res 1999;32:350.
4. Spiro TG, Kozlowski PM. J Biolog Inorg Chem JBIC 1997;2:516.A *JBIC* commentary has appeared. *J. Biolog. Inorg. Chem. JBIC*, **1997**, 515–552. The parts are: (a)Slebodnick C, Ibers JA. *J Biolog Inorg Chem JBIC* 1997;2:521.(b)Vangberg T, Bocian DF, Ghosh A. *J Biolog Inorg Chem JBIC* 1997;2:526.(c)Lim M, Jackson TA, Anfinrud PA. *J Biolog Inorg Chem JBIC* 1997;2:531.(d)Sage JT. *J Biolog Inorg Chem JBIC* 1997;2:537.(e)Olson JS, Phillips GN Jr. *J Biolog Inorg Chem JBIC* 1997;2:544.(f)
5. Kachalova, GS.; Popov, AN.; Bartunik, HD. Science. Washington, D.C; 1999. p. 284-473.
6. Einsle O, Messerschmidt A, Huber R, Kroneck PMH, Neese F. J Am Chem Soc 2002;124:11737. [PubMed: 12296741]
7. Quillin ML, Arduini RM, Olson JS, Phillips GN Jr. J Mol Biol 1993;234:140. [PubMed: 8230194]
8. Kuriyan J, Wilz S, Karplus M, Petsko GA. J Mol Biol 1986;192:133. [PubMed: 3820301]
9. Vojtechivský J, Chu K, Berendzen J, Sweet RM, Schlichting I. Biophys J 1999;2153. [PubMed: 10512835]
10. Peng SM, Ibers JA. J Am Chem Soc 1976;98:8032. [PubMed: 993515]
11. Salzmann R, Ziegler CJ, Godbout N, McMahon MT, Suslick KS, Oldfield E. J Am Chem Soc 1998;120:11323.
12. Salzmann R, McMahon MT, Godbout N, Sanders LK, Wojdelski M, Oldfield E. J Am Chem Soc 1999;121:3818.
13. Scheidt WR, Haller KJ, Fons M, Mashiko T, Reed CA. Biochemistry 1981;20:3653. [PubMed: 7260062]
14. Caron C, Mitschler A, Rivière G, Ricard L, Schappacher M, Weiss R. J Am Chem Soc 1979;101:7401.
15. Ricard L, Weiss R, Momenteau M. J Chem Soc, Chem Commun 1986:818.
16. Kim K, Fettinger J, Sessler JL, Cyr M, Hugdahl J, Collman JP, Ibers JA. J Am Chem Soc 1989;111:403.
17. Kim K, Ibers JA. J Am Chem Soc 1991;113:6077.
18. Slebodnick C, Duval ML, Ibers JA. Inorg Chem 1996;35:3607.
19. Slebodnick C, Fettinger JC, Peterson HB, Ibers JA. J Am Chem Soc 1996;118:3216.
20. Nasri H, Wang Y, Huynh BH, Scheidt WR. J Am Chem Soc 1991;113:717.
21. Nasri H, Ellison MK, Chen S, Huynh BH, Scheidt WR. J Am Chem Soc 1997;119:6274.
22. Nasri H, Ellison MK, Krebs C, Huynh BH, Scheidt WR. J Am Chem Soc 2000;122:10795.
23. Nasri H, Goodwin JA, Scheidt WR. Inorg Chem 1990;29:185.
24. Nasri H, Wang Y, Huynh BH, Walker FA, Scheidt WR. Inorg Chem 1991;30:1483.
25. Nasri H, Haller KJ, Wang Y, Huynh BH, Scheidt WR. Inorg Chem 1992;31:3459.
26. Ellison MK, Schulz CE, Scheidt WR. Inorg Chem 1999;38:100.
27. Abbreviations: Porph, a generalized porphyrin dianion; *Tp*-OCH₃PP, dianion of *meso*-tetra-*p*-methoxyphenylporphyrin; TPP, dianion of *meso*-tetraphenylporphyrin; TMP, *meso*-tetramesitylporphyrin; OEP, dianion of 2,3,7,8,12,13,17,18-octaethylporphyrin; Deut, deuteroporphyrin IX dimethyl ester; TpivPP, dianion of ($\alpha,\alpha,\alpha,\alpha$ -tetrakis(*o*-pival-amidophenyl)

porphyrin; TPPiv₂C₁₂P, dianion of 5,15-[2,2'-(dodecanediamido)diphenyl]- α,α -10,20-bis(*o*-pivaloylaminophenylporphyrin; β -PocpivP, dianion of “pocket” porphyrin; C₂-Cap and C₃-Cap, dianion of “capped” porphyrins; OC₃OPor, dianion of “benzene capped” porphyrin; PMS, pentamethylene sulfide; Py, pyridine; THT, tetrahydrothio-phene; THF, tetrahydrofuran; HIm, imidazole; 1-MeIm, 1-methylimidazole; 2-MeHIm, 2-methylimidazole; 1,2-Me₂Im, 1,2-dimethylimidazole; 4-NMe₂Py, 4-N-dimethylamino-pyridine; Pip, piperidine; 4-MePip, 4-methylpiperidine; Pz, pyrazole; 1-VinIm, 1-vinyl-imidazole; 1-BzIM, 1-benzylimidazole; 1-AcIM, 1-acetylimidazole; Iz, indazole (benzo-pyrazole); SC₆HF₄, 2,3,5,6-tetrafluorophenyl thiolate; SPh, phenyl thiolate; PMe₃, trimethyl phosphine; Kryptofix-222 or 222, 4,7,13,16,21,24-hexaoxo-1,10-diazabicyclo-[8.8.8]hexacosane; N_p, porphyrinato nitrogen.

28. Finnegan MG, Lappin AG, Scheidt WR. Inorg Chem 1990;29:181.
29. Armagero, WLF.; Perrin, DD. Purification of Laboratory Chemicals. 4th ed. Woburn, MA: Butterworth-Heinemann; 1997. p. 140
30. Collman JP, Gagne RR, Halbert TR, Lang G, Robinson WT. J Am Chem Soc 1975;97:1427. [PubMed: 1133392]
31. Gismelseed A, Bominaar EL, Bill E, Trautwein AX, Winkler H, Nasri H, Doppelt P, Mandon D, Fischer J, Weiss R. Inorg Chem 1990;29:2741.
32. Scheidt WR, Turowska-Tyrk I. Inorg Chem 1994;33:1314.
33. Sheldrick GM. Acta Crystallogr 1990;A46:467.
34. Sheldrick GM. J Appl Cryst. in preparation.
35. $R_1 = \sum ||F_o - |F_c|| / \sum |F_o|$ and $wR_2 = \{ \sum [w(F_o^2 - F_c^2)^2] / \sum [wF_o^4] \}^{1/2}$ The conventional R-factors R_1 are based on F, with F set to zero for negative F_c^2 . The criterion of $F^2 > 2\sigma(F^2)$ was used only for calculating R_1 R-factors based on F^2 (wR_2) are statistically about twice as large as those based on F, and R-factors based on ALL data will be even larger.
36. Scheidt WR, Frisse ME. J Am Chem Soc 1975;97:17. [PubMed: 1133330]
37. Mu XH, Kadish KM. Inorg Chem 1988;27:4720.
38. Wayland BB, Mehne LF, Swartz J. J Am Chem Soc 1978;100:2379.
39. Scheidt WR, Piciulo PL. J Am Chem Soc 1976;98:1913. [PubMed: 1254850]
40. Wyllie, GRA.; Schulz, CE.; Scheidt, WR. Inorg Chem. in press
41. Safo MK, Scheidt WR, Gupta GP. Inorg Chem 1990;29:626.
42. Ellison, M. K.; Scheidt, W. R., unpublished results.
43. Collman JP, Brauman JI, Doxsee KM, Halbert TR, Bunnenberg E, Linder RE, LaMar GN, Del Guadio J, Lang G, Spartalian K. J Am Chem Soc 1980;102:4182.
44. Mandon D, Ott-Woelfel F, Fisher J, Weiss R, Bill E, Trautwein AX. Inorg Chem 1990;29:2442.
45. Roth, A.; Scheidt, W. R., unpublished results.
46. Schappacher, M. Thesis. Université de Strasbourg; Strasbourg, France: 1982. Ph. D
47. Yoshimura T. Inorg Chim Acta 1984;83:17.
48. Stolzenberg AM, Strauss SH, Holm RH. J Am Chem Soc 1981;103:4763.
49. Rougee M, Brault D. Biochemistry 1975;14:4100.
50. Wang CM, Brinigar WS. Biochemistry 1979;18:4960. [PubMed: 508726]
51. All other five-coordinate iron(II) porphyrinates with a single anionic axial ligand are high spin. Some examples include the anions ethanethiolate,⁵² chloride,⁵³ tetrafluorophenyl-thiolate,⁵³ phenoxide,⁵⁴ 2-methylimidazolate,⁴⁴ and acetate.⁵⁵
52. Schappacher M, Ricard L, Fischer J, Weiss R, Montiel-Montoya R, Bill E, Trautwein AX. Inorg Chem 1989;28:4639.
53. Schappacher M, Ricard L, Weiss R, Montiel-Montoya R, Gonser U, Bill E, Trautwein AX. Inorg Chim Acta 1983;78:L9.
54. Nasri H, Fischer J, Weiss R, Bill E, Trautwein AX. J Am Chem Soc 1987;109:2549.
55. Bominaar EL, Ding X, Gismelseed A, Bill E, Winkler H, Trautwein AX, Nasri H, Fischer J, Weiss R. Inorg Chem 1992;31:1845.
56. The large change in Fe–N(NO)₂ bond length is not merely a result of change in coordination number. See reference 22 for a detailed discussion.

57. The only exceptions are two isomorphous forms of $[\text{Fe}(\text{TpivPP})(\text{NO}_2)(\text{NO})]$ for which the synthesis was designed to place the anionic ligand on the open face. The actual result was disorder of the axial ligands with a 57% occupancy of a nitro group on the open face of the picket fence porphyrin and a linear nitrosyl group inside the pocket. In the second case there was a 26% occupancy of the nitro out of the pocket.²⁶
58. Safo MK, Nesson MJM, Walker FA, Debrunner PG, Scheidt WR. *J Am Chem Soc* 1997;119:9438.
59. Kobayashi H, Maeda Y, Yanagawa Y. *Bull Chem Soc Jpn* 1970;43:2342.
60. Dolphin D, Sams JR, Tsin TB, Wong KL. *J Am Chem Soc* 1976;98:6970. [PubMed: 965659]
61. Collman JP, Hoard JL, Kim N, Lang G, Reed CA. *J Am Chem Soc* 1975;97:2676. [PubMed: 166106]
62. Polam JR, Wright JL, Christensen KA, Walker FA, Flint H, Winkler H, Grodzicki M, Trautwein AX. *J Am Chem Soc* 1996;118:5272.
63. Havlin RH, Godbout N, Salzmann R, Wojdelski M, Arnold W, Schulz CE, Oldfield E. *J Am Chem Soc* 1998;120:3144.
64. Conner WM, Straub DK. *Inorg Chem* 1976;15:2289.
65. Maeda Y, Harami T, Morita Y, Trautwein AX, Gonser U. *J Chem Phys* 1981;75:36.
66. Cao C, Dahal S, Shang M, Beatty AM, Hibbs W, Schulz CE, Scheidt WR. *Inorg Chem* 2003;42:5202. [PubMed: 12924891]
67. Bohle DS, Debrunner P, Fitzgerald J, Hansert B, Hung CH, Thompson AJ. *J Chem Soc, Chem Commun* 1997:91.
68. Wyllie GRA, Scheidt WR. *Inorg Chem* 2003;42:4259. [PubMed: 12844295]
69. Ellison MK, Schulz CE, Scheidt WR. *Inorg Chem* 2000;39:5102. [PubMed: 11233208]
70. Ellison MK, Schulz CE, Scheidt WR. *J Am Chem Soc* 2002;124:13833. [PubMed: 12431114]
71. Schünemann V, Benda R, Trautwein AX, Walker FA. *Isr J Chem* 2000;40:9.
72. Settin MF, Fanning JC. *Inorg Chem* 1988;27:1431.
73. Richter-Addo GB, Wheeler RA, Hixson CA, Chen L, Khan MA, Ellison MK, Schulz CE, Scheidt WR. *J Am Chem Soc* 2001;123:6314. [PubMed: 11427056]
74. Paulsen H, Krockel M, Grodzicki M, Bill E, Trautwein AX, Leigh GJ, Silver J. *Inorg Chem* 1995;34:6244.
75. The quadrupole splittings (ΔE_Q) for the two geometric forms of $[\text{Fe}(\text{TpivPP})(\text{NO}_2)(\text{NO})]^-$ are significantly different. Although the Mössbauer spectra for the two forms were taken at two different temperatures, any temperature-dependent effect on ΔE_Q is unlikely to make the two values more equivalent.
76. Li M, Bonnet D, Bill E, Neese F, Weyhermüller T, Blum N, Sellman D, Wieghardt K. *Inorg Chem* 2002;41:3444. [PubMed: 12079463]
77. Neese F. *Inorg Chim Acta* 2002;337:181.

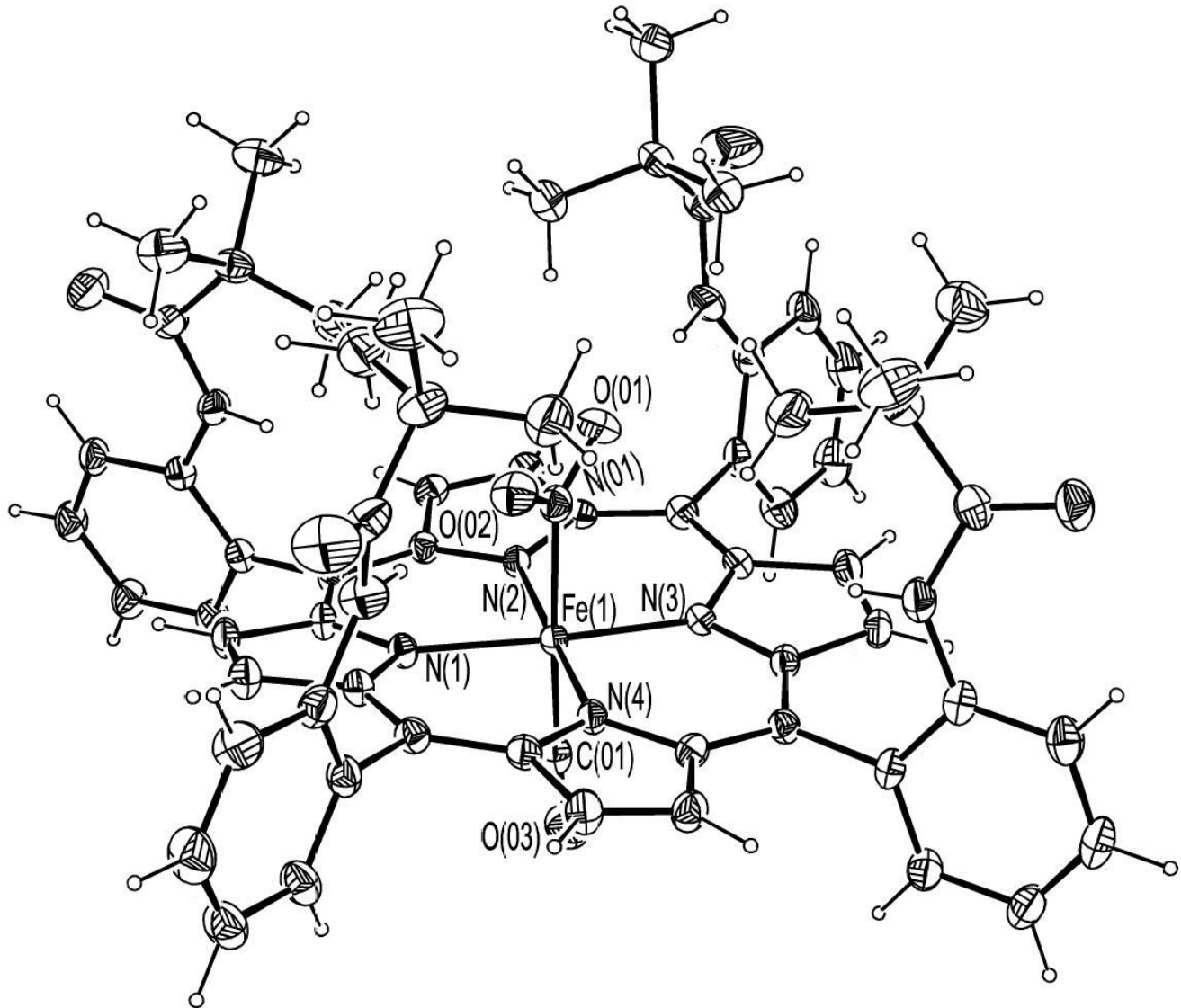
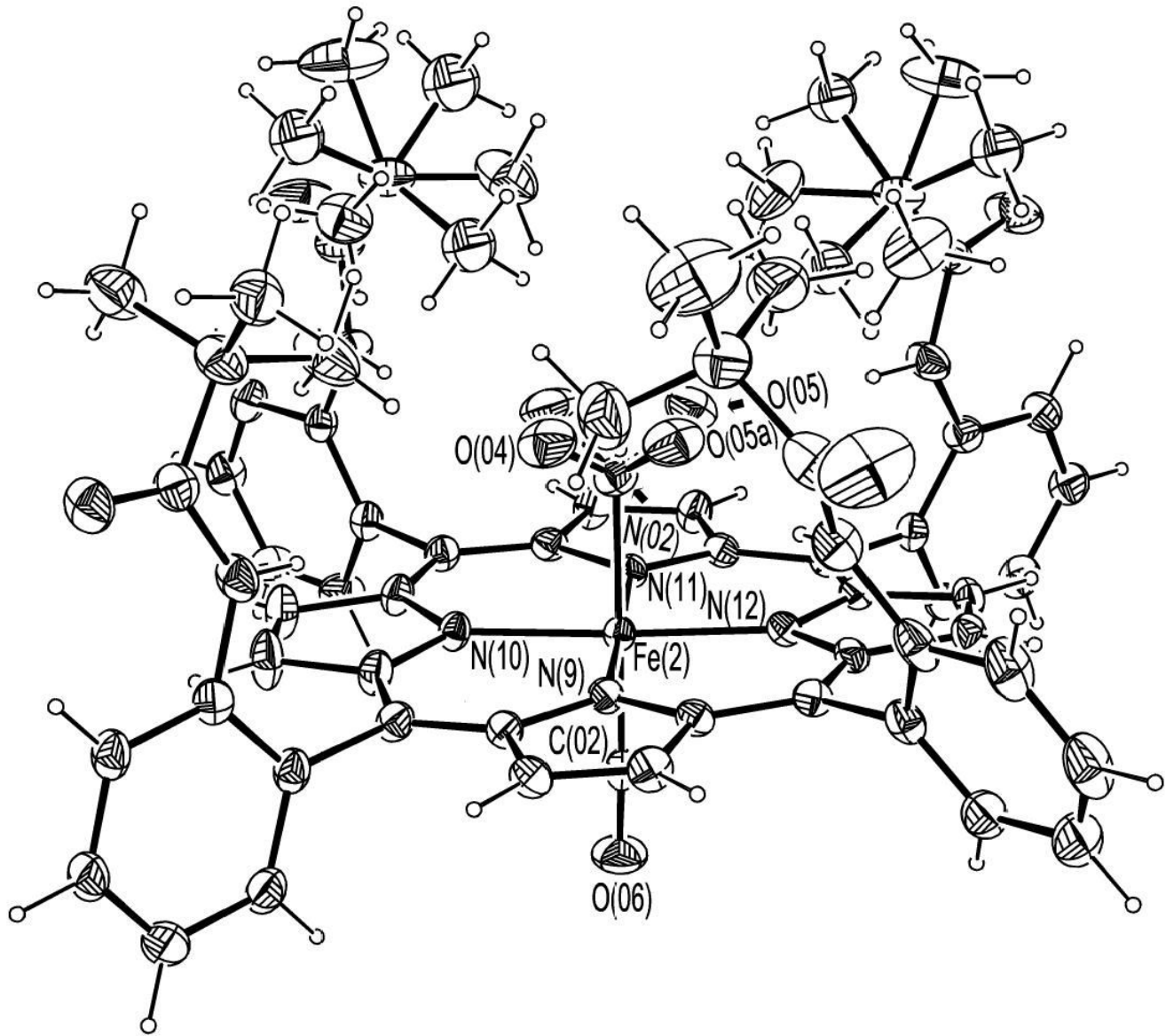
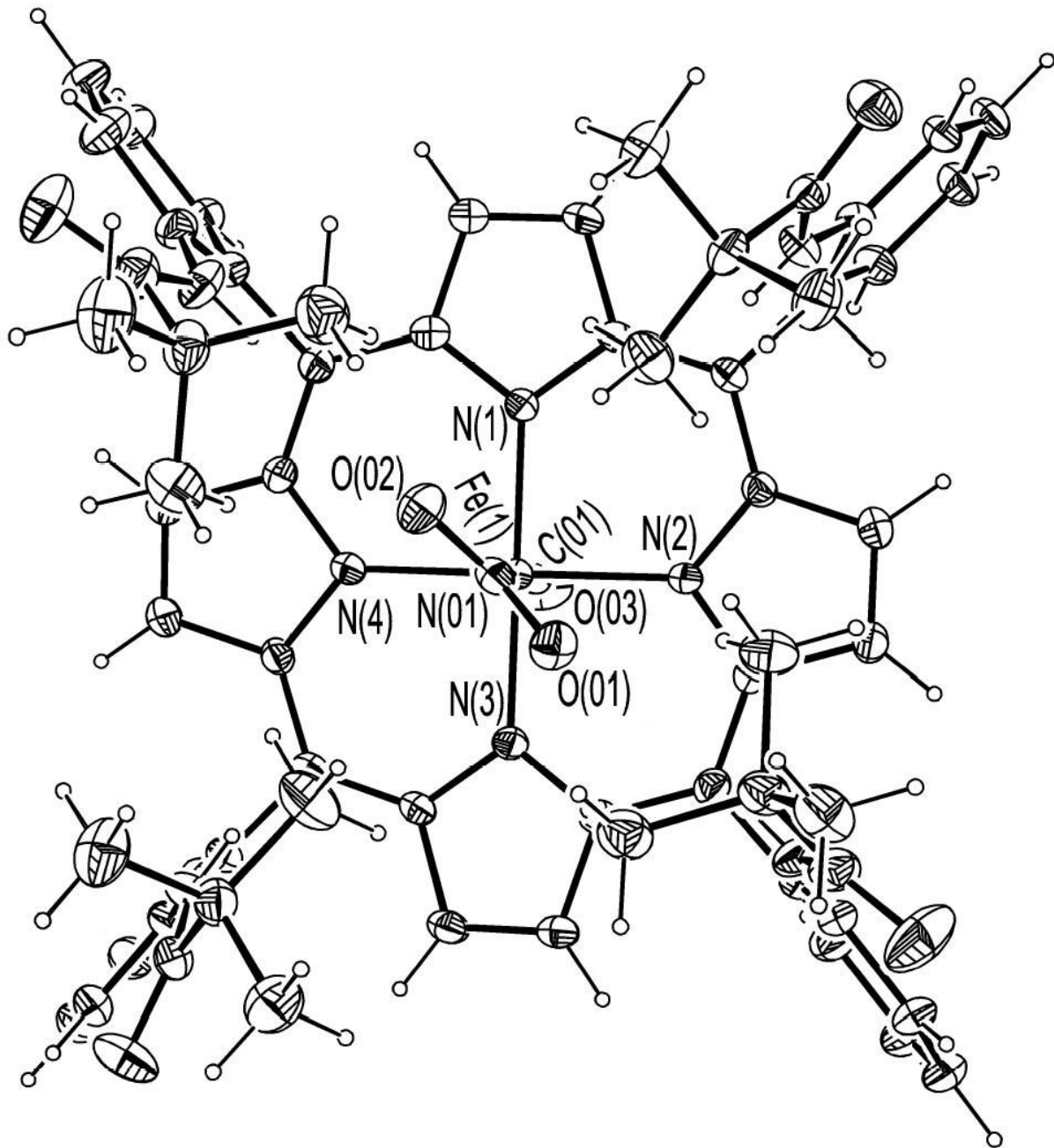


Figure 1.

ORTEP diagram of $[\text{Fe}(\text{TpivPP})(\text{NO}_2)(\text{CO})]^-$ (**1**) showing the coordination at iron. 50% probability ellipsoids are depicted.

**Figure 2.**

ORTEP diagram of $[\text{Fe}(\text{TpivPP})(\text{NO}_2)(\text{CO})]^-$ (**2**). 50% probability ellipsoids are depicted. The rotational disorder in the nitro group and the pivalamide groups are shown.

**Figure 3.**

ORTEP diagram of $[\text{Fe}(\text{TpivPP})(\text{NO}_2)(\text{CO})]^-$ (1) looking down on the porphyrin plane.

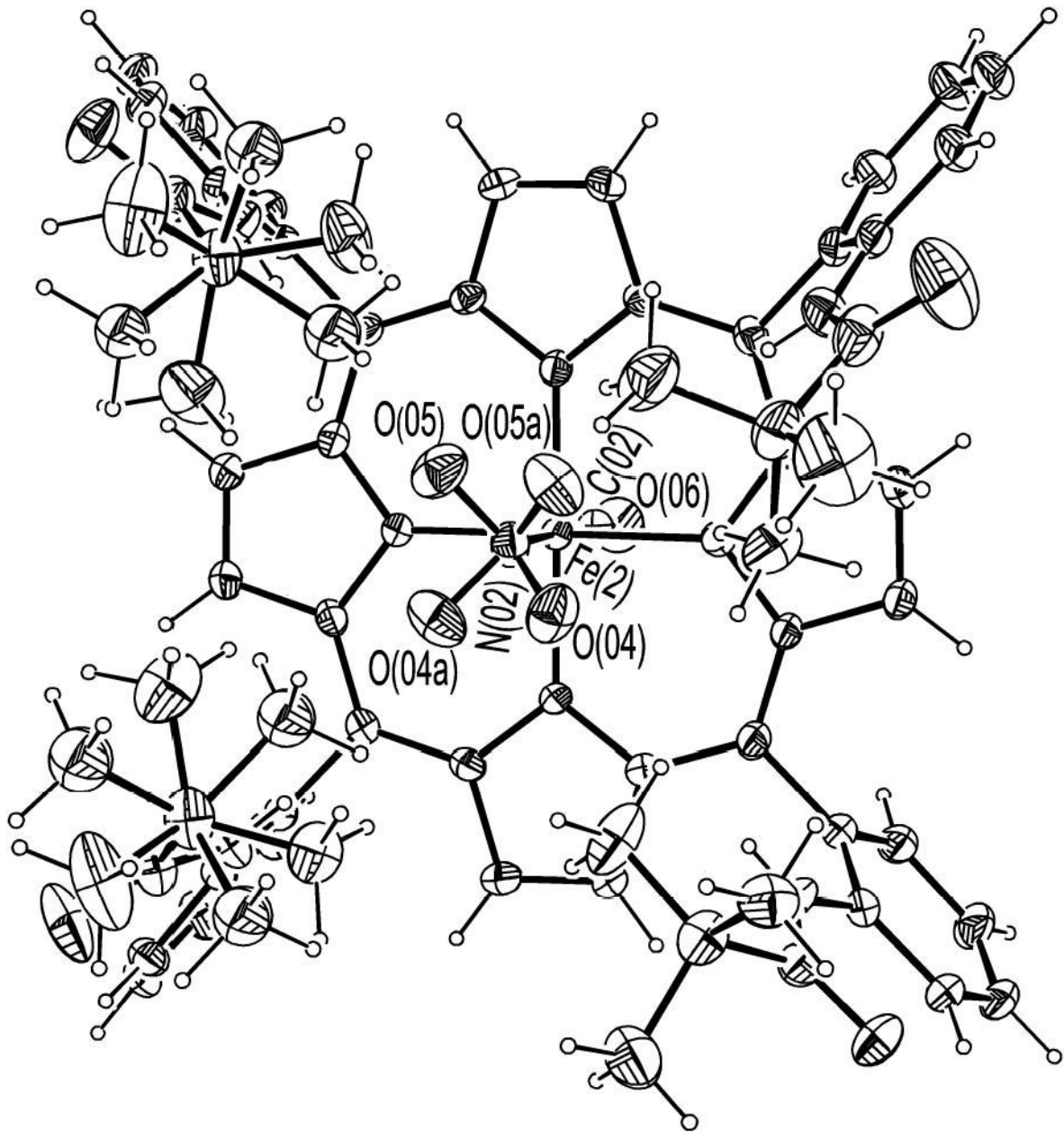


Figure 4.
ORTEP diagram of $[\text{Fe}(\text{TpivPP})(\text{NO}_2)(\text{CO})]^-$ (2) looking down on the porphyrin plane.

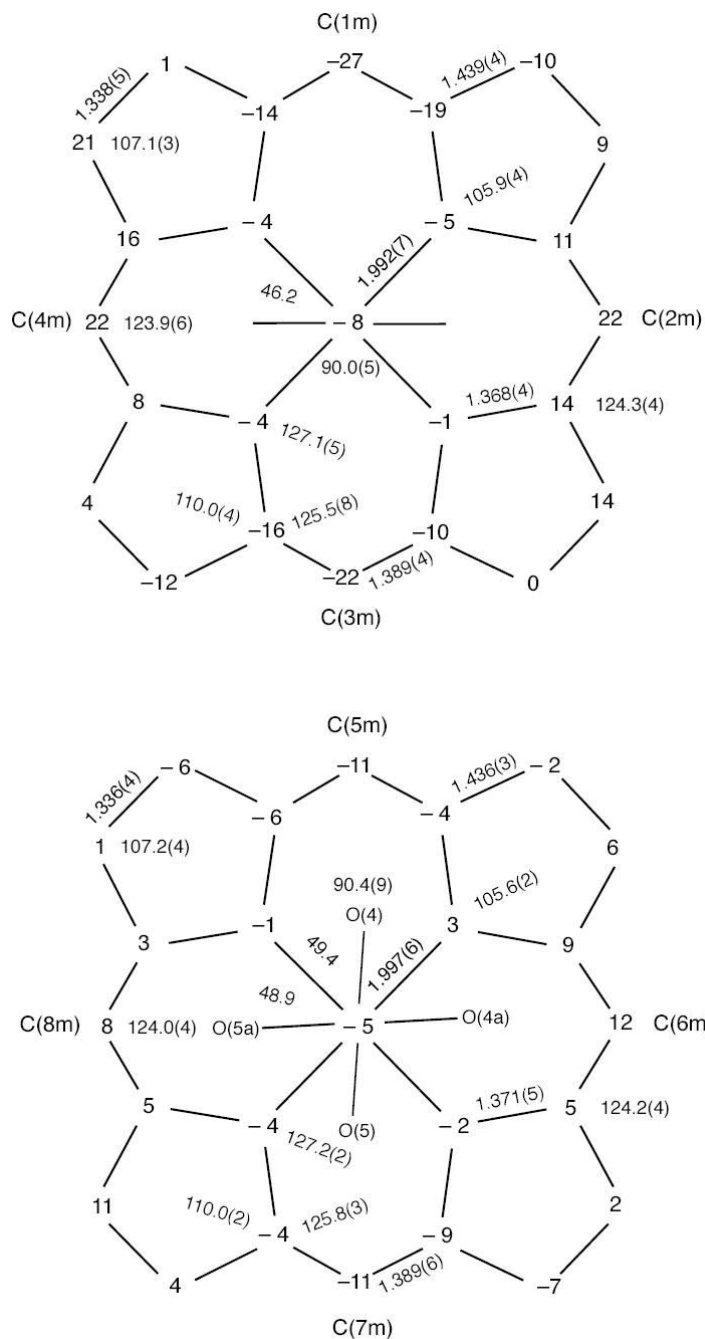


Figure 5.

Formal diagrams of the porphyrinato cores of $[\text{Fe}(\text{T pivPP})(\text{NO}_2)(\text{CO})]^-$ (**1**) (top) and $[\text{Fe}(\text{T pivPP})(\text{NO}_2)(\text{CO})]^-$ (**2**) (bottom). Illustrated are the displacements of each atom from the mean plane of the 24-atom porphyrin cores in units of 0.01 Å. Positive values of displacement are toward the NO_2 ligand in each anion. The major orientation (54%) of the nitrite in anion **2** is the horizontal orientation. The diagram also gives the averaged values of each distinct bond distance and angle in the porphyrinato cores.

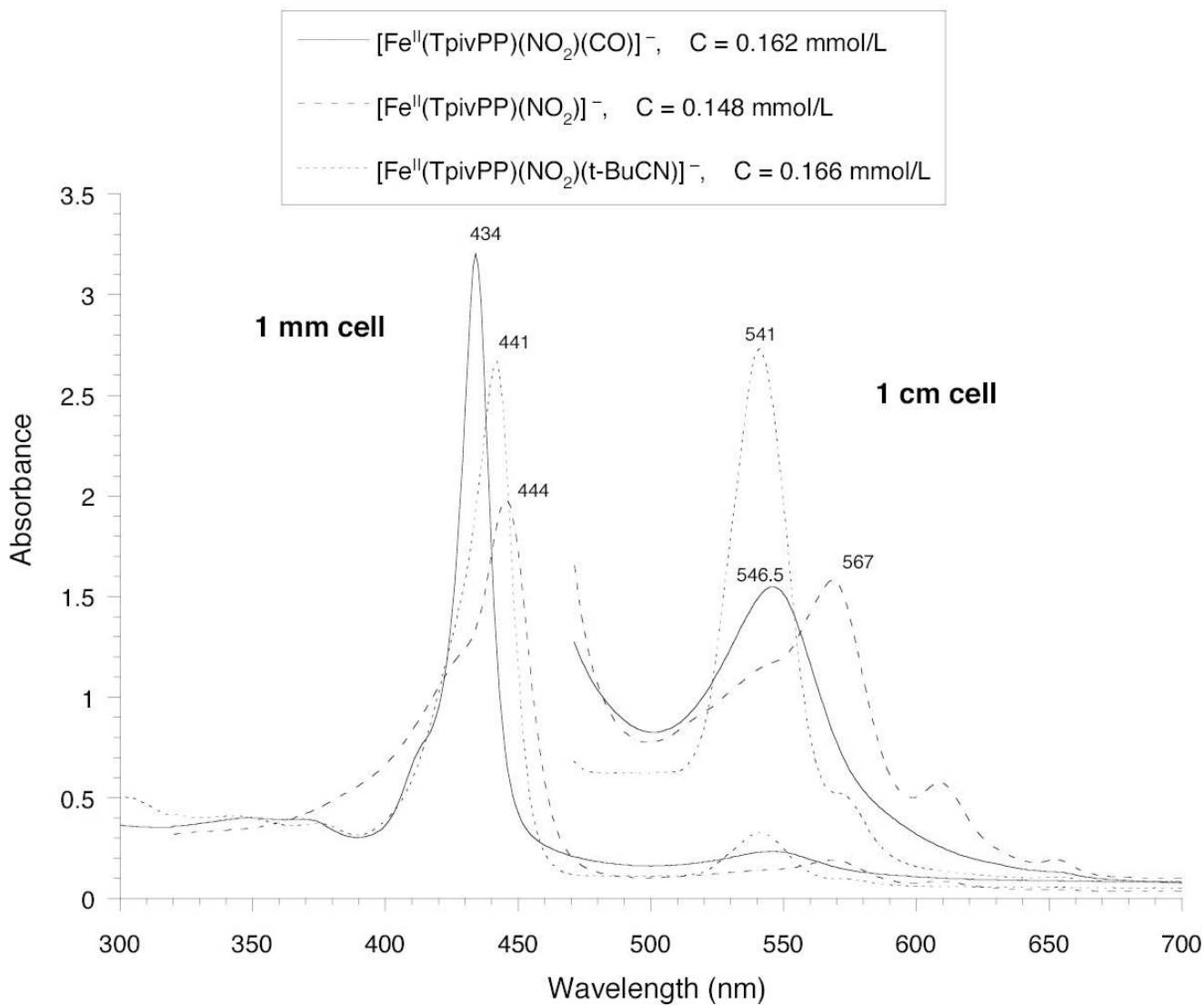


Figure 6.

UV-vis spectra of $[\text{Fe}(\text{TpivPP})(\text{NO}_2)]^-$, $[\text{Fe}(\text{TpivPP})(\text{NO}_2)(\text{CO})]^-$, and $[\text{Fe}(\text{TpivPP})(\text{NO}_2)(t\text{-BuNC})]^-$ taken under argon in chlorobenzene.

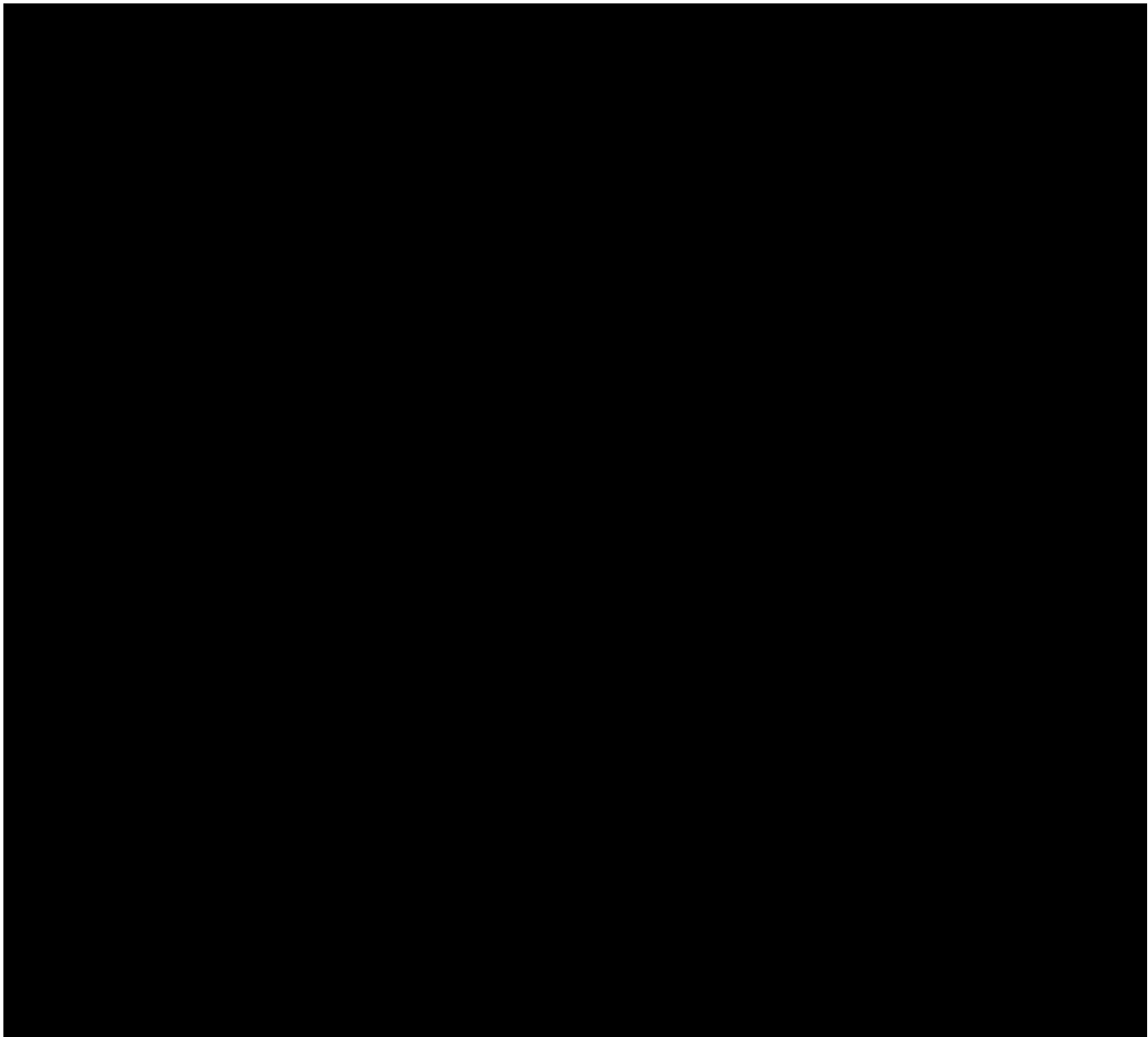


Figure S1.
ORTEP diagram of the K(222) cryptand, cation **1**.

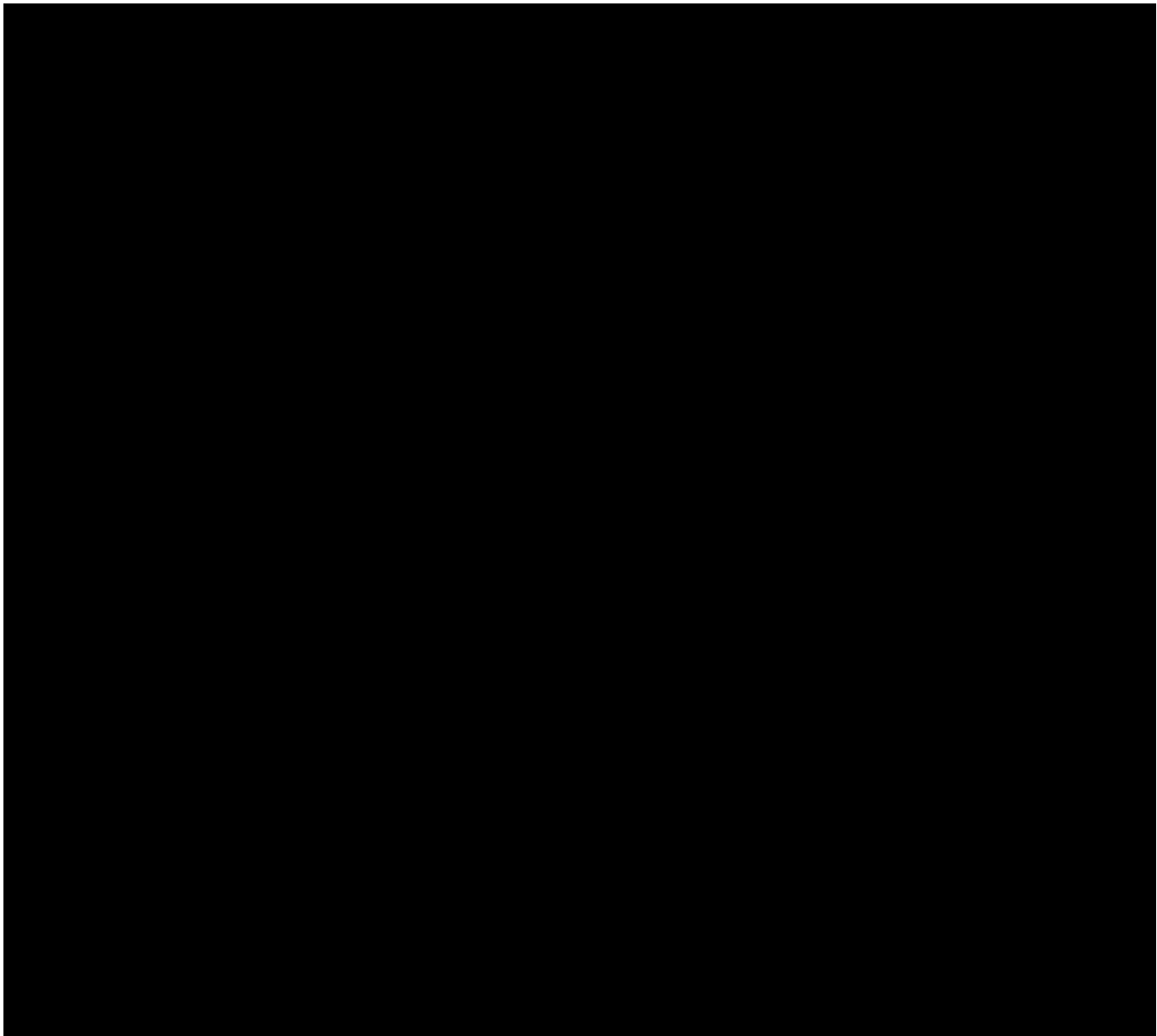
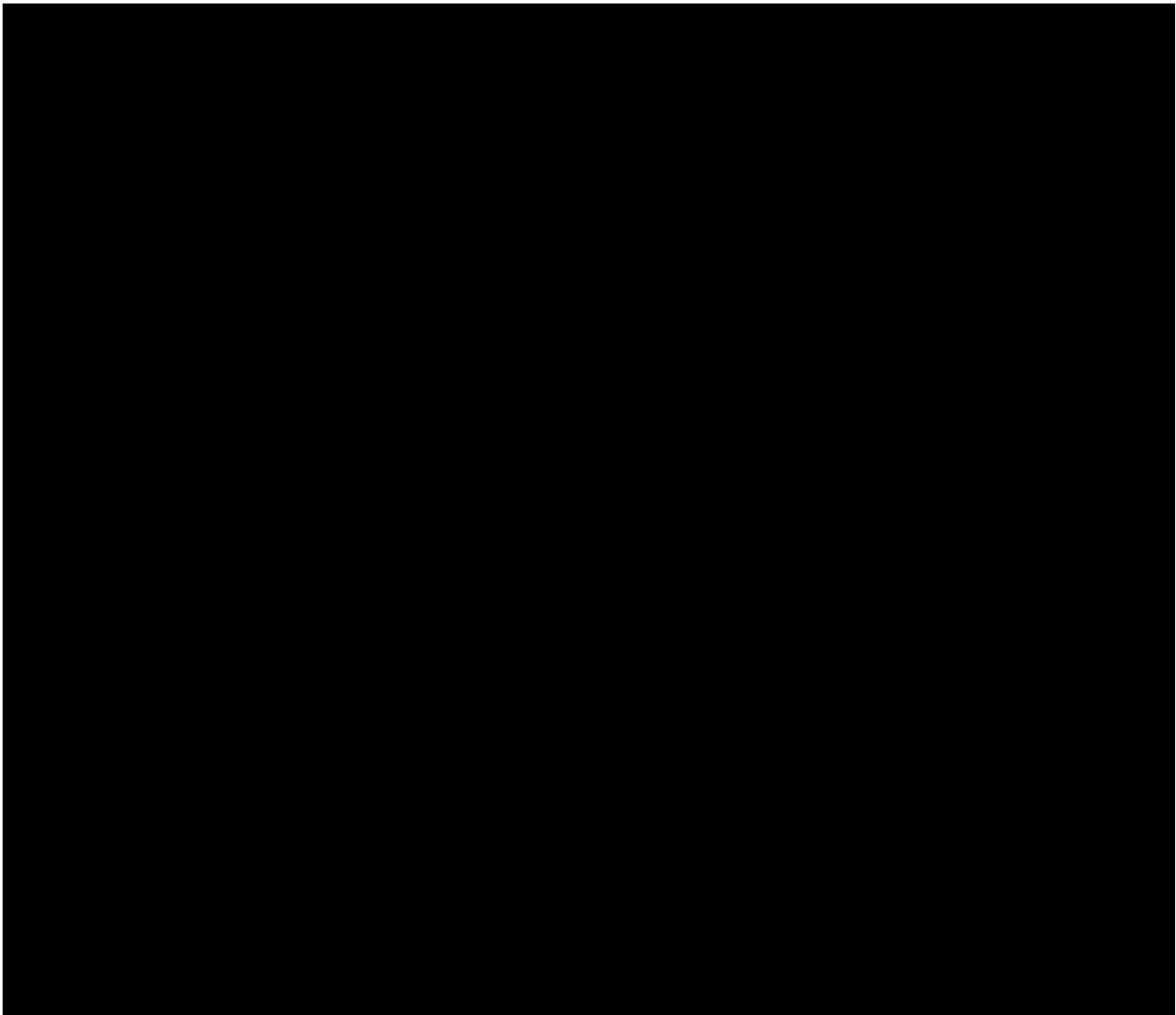
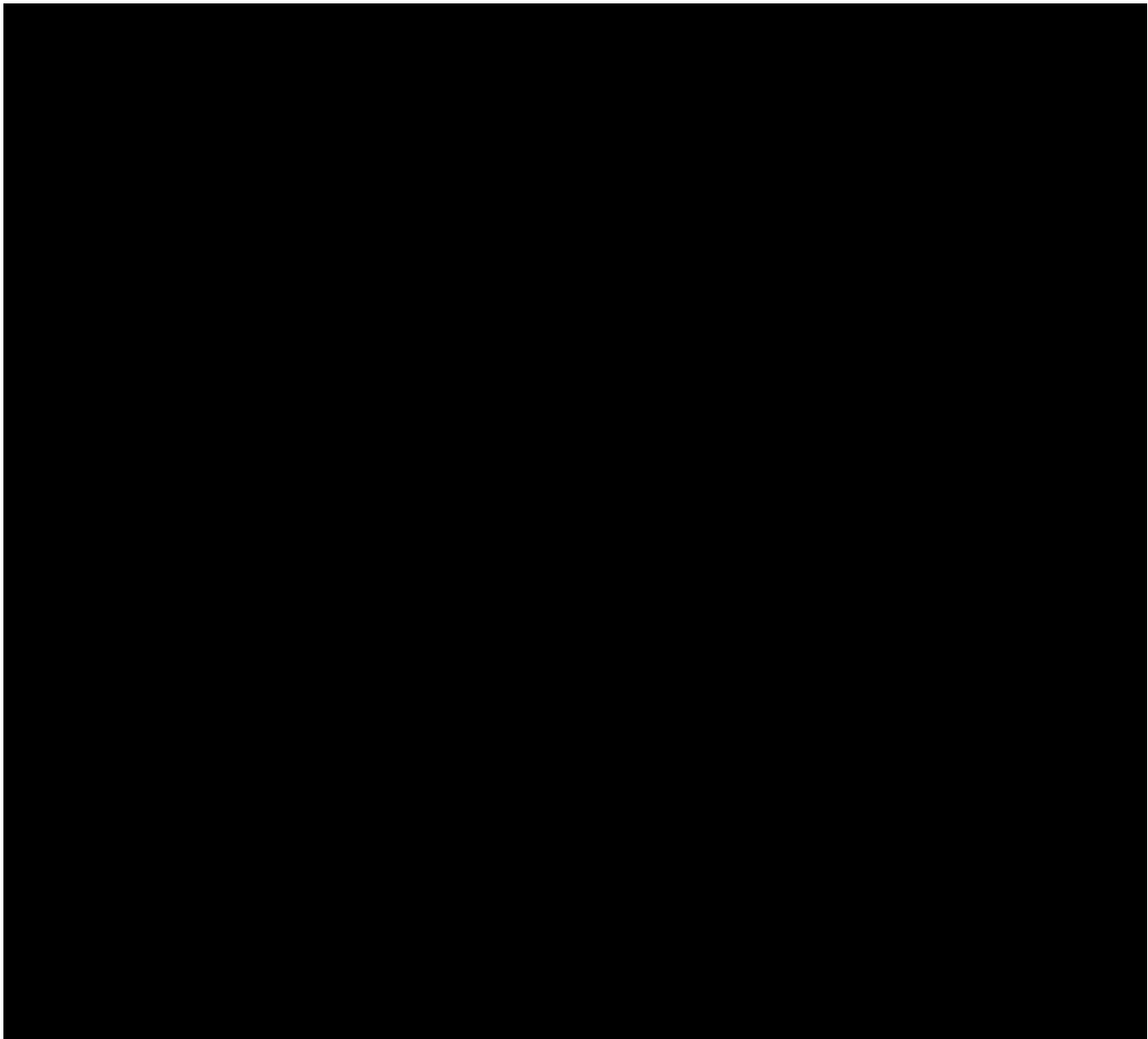


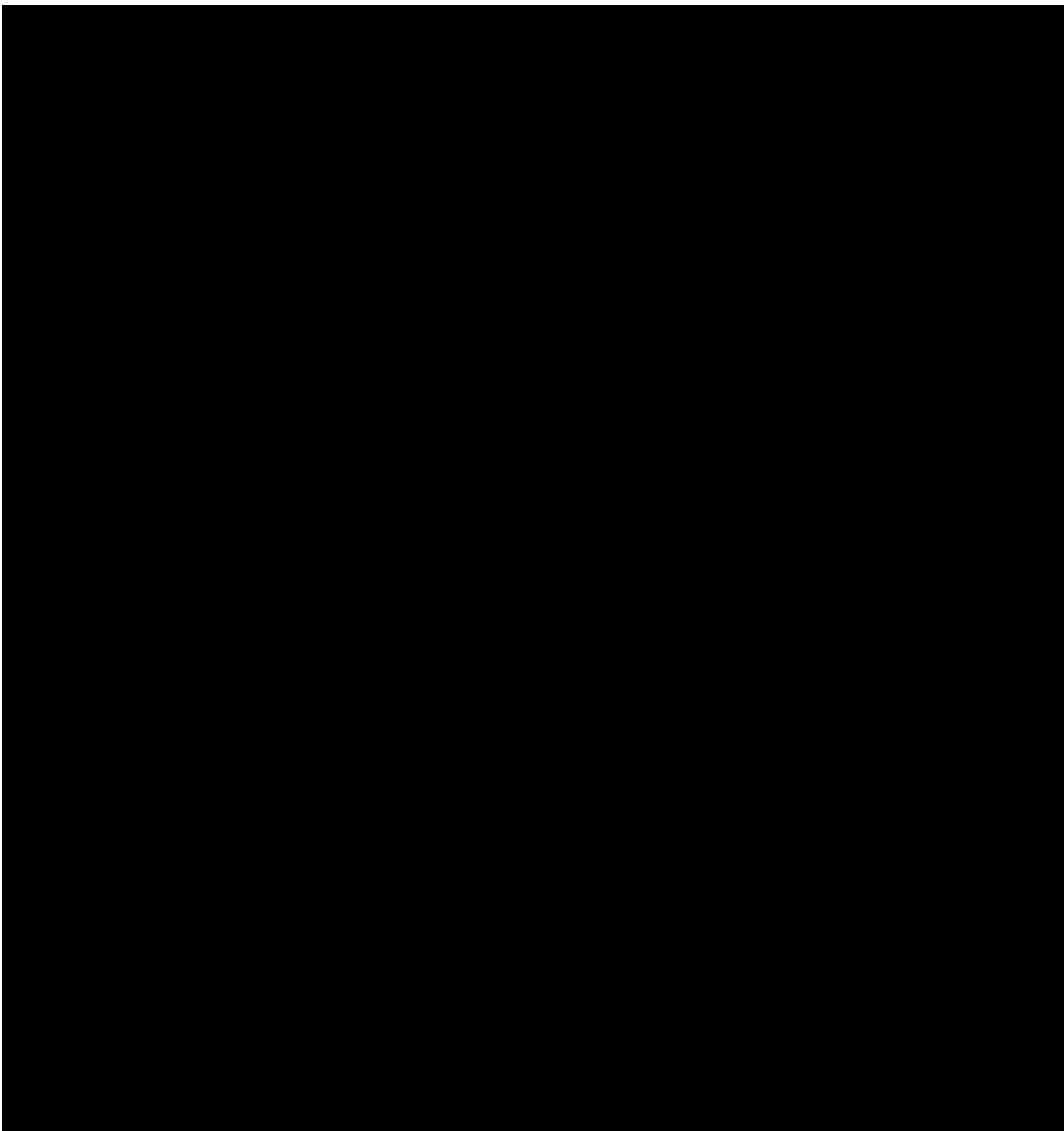
Figure S2.
ORTEP diagram of the K(222) cryptand, cation **2**.

**Figure S3.**

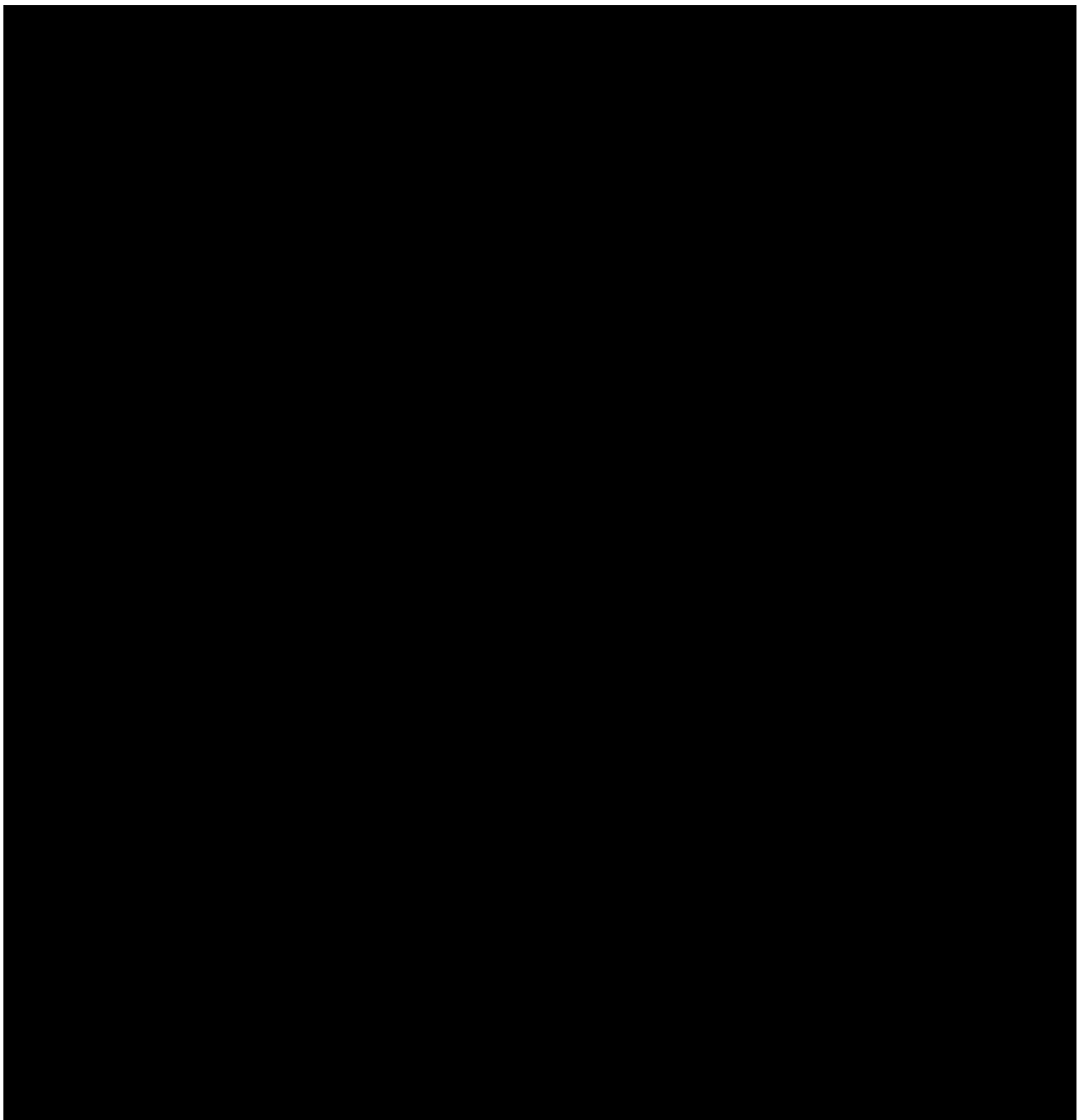
ORTEP diagram of $[\text{Fe}(\text{TpivPP})(\text{NO}_2)(\text{CO})]^-$ (**1**) showing the coordination at iron. 50% probability ellipsoids are depicted and all atomic label are given.

**Figure S4.**

ORTEP diagram of $[\text{Fe}(\text{TpivPP})(\text{NO}_2)(\text{CO})]^-$ (2). 50% probability ellipsoids are depicted. The rotational disorder in the nitro group and the pivalamide groups are shown.

**Figure S5.**

ORTEP of $[\text{Fe}(\text{TpiVPP})(\text{NO}_2)(\text{CO})]^-$ (**1**) looking down on the porphyrin plane.

**Figure S6.**

ORTEP of $[\text{Fe}(\text{TpiVPP})(\text{NO}_2)(\text{CO})]^-$ (**2**) looking down on the porphyrin plane.

Table 1Crystallographic details for [K(222)][Fe(TpivPP)(NO₂)(CO)]·1/2C₆H₅Cl

formula	C ₈₉ H ₁₀₅ ClFeKN ₁₁ O ₁₃
FW	1667.24
<i>a</i> , Å	33.548(6)
<i>b</i> , Å	18.8172(15)
<i>c</i> , Å	27.187(2)
β, deg	95.240(7)
<i>V</i> , Å ³	17091(4)
<i>Z</i>	8
space group	<i>P</i> 2 ₁ /c
<i>D</i> _c , g/cm ³	1.296
<i>F</i> (000)	7056
μ, mm ⁻¹	0.325
crystal dimens, mm	0.24 × 0.12 × 0.08
absorption correction	DIFABS
λ, Å	0.71073
<i>T</i> , K	130(2)
total data colld	52417
unique data	32440 (<i>R</i> _{int} = 0.0759)
unique obsd data [<i>I</i> > 2 σ(<i>I</i>)]	21632
refinement method	on F ² (SHELXL)
final <i>R</i> indices [<i>I</i> > 2 σ(<i>I</i>)]	<i>R</i> ₁ = 0.0775, <i>wR</i> ₂ = 0.1850
final <i>R</i> indices [for all data]	<i>R</i> ₁ = 0.1224, <i>wR</i> ₂ = 0.2200

Table 2Electronic Spectral Data for Selected Iron(II) and Iron(III) Tetraarylporphyrins ^a

Complex	Soret region (log ϵ)	λ_{max} (nm)		α, β region (log ϵ)	ref.	
[Fe(TPP)(NO)] ^b	406 (4.97)	475(sh)	Five-Coordinate Iron(II) 538 (4.00)	604 (3.45)	36	
[Fe(TpivPP) (NO)] ^c	407 (5.15)	477 (sh) (4.35)	539 (4.12)	607 (3.62)	25	
[Fe(TMP) (NO)] ^d	408 (4.96)	477(sh)	539 (3.04)	611 (3.84)	37	
[Fe(TPP)(CO)] ^e	419		537	570	~610	38
[Fe(TpivPP) (NO ₂) ^{-c}	433(sh) (4.94)	444 (5.12)	543 (sh) (3.89)	567 (4.02)	608 (3.59)	20, 22
[Fe(TpivPP) (NO ₂)(CO)] ^{-c}	414 (sh) (4.67)	434 (5.30)	Six-Coordinate Iron(II) Nitro 546 (3.98)		tw	
[Fe(TpivPP) (NO ₂) ^{-c}		441 (5.52)	541 (4.20)	572 (3.45)	tw	
BuNC)] ^{-c}						
[Fe(TpivPP) (NO ₂)(NO)] ^{-c}		433 (5.17)	543 (4.14)		21	
[Fe(TpivPP) (NO ₂)(Py)] ^{-c}	413(sh) (4.83)	430 (5.23)	533 (4.21)	560 (sh) (3.66)	653 (2.83)	22
[Fe(TpivPP) (NO ₂) ^{-c} (PMS)] ^{-c}	418(sh) (4.88)	432 (5.07)	537 (4.18)	558 (sh) (3.81)	653 (3.12)	22
[Fe(TPP)(1-MeIm)(NO)] ^b	415 (5.26)	460 (4.26)	Six-Coordinate Iron(II) Other 545 (3.99)	580 (sh) (3.78)	643 (3.05)	39
[Fe(TPP)(4-NMe ₂ Py) (NO)] ^d	416		554	586		40
[Fe(TPP)(1-MeIm)(NO)] ^d	416		543	583	641	40
[Fe(TPP)(4-MePip)(NO)] ^d	417	463	554	591		40
[Fe(TPP)(1-VinIm) ₂] ^d	424 (5.22)		533 (4.24)	564 (3.67)		41
[Fe(TPP)(1-BzIm) ₂] ^d	426 (5.23)		533 (4.24)	565 (3.63)		41
[Fe(TPP)(1-AcIm) ₂] ^d	422 (5.14)		533 (3.99)	563 (3.62)		41
[Fe(TPP)(1-MeIm) ₂] ^d	425 (5.09)		533 (4.26)	564 (3.75)		41
[Fe(TpivPP)(1-MeIm) ₂] ^c	430		536			42
[Fe(TpivPP)(1-MeIm) ₂] ^e	432 (5.36)		537 (4.32)	562(sh)		43
[Fe(TpivPP)(Im ⁻)(HIm)] ^{-c}	442 (4.00)		544 (3.47)			44
[Fe(TPP)(1-MeIm)(CO)] ^e	427 (5.50)		542 (3.95)			43
[Fe(TPP)(1-MeIm)(CO)] ^d	422		544			45
[Fe(TpivPP)(1-MeIm)(CO)] ^c	425		542			42
[Fe(TPP)(CO) ₂] ^e	426		551	578		38
[Fe(TpivPP)(SEt)] ^{-c}	421		Iron(II) Thiolates 533	575	625	46
[Fe(TpivPP)(SEt)(CO)] ^{-c}	392,467		565	612		46
[Fe(TpivPP)(SPh)] ^{-c}	421		536	575	625	46

Complex		Soret region (log ϵ)	λ_{\max} (nm)	α, β region (log ϵ)	ref.
[Fe(TpivPP) (SPh)(CO)] ^c		403,464	555	605	46
[Fe(TpivPP) (NO ₂) ₂] ^c	364(sh)	426 (5.11)	Six-Coordinate Iron(III) Nitro 464(sh) 553 (4.15)		23
[Fe(TpivPP) (NO ₂)(Py)] ^c		422 (5.26)	459 (sh) 550 (4.11)		24
[Fe(TPP) (NO ₂)(NO)] ^b		433 (5.34)	510 (sh) (3.70) 545 (4.20)	577 (sh) (3.70)	47
[Fe(Tp- OCH ₃ PP) (NO ₂)(NO)] ^c		437		549 586	26
[Fe(TpivPP) (NO ₂)(NO)] ^e		433		543 581	26

^aAll spectra were taken at 25°C.

^bChloroform solution.

^cChlorobenzene solution.

^dDichloromethane solution.

^eToluene solution.

Table 3
Bond Distances (\AA) for (Nitro)iron Porphyrin Derivatives

Iron(II) Complex	Fe–N _p	Fe–N _{NO₂}	Fe–L	ref.
[Fe(TpivPP)(NO ₂)(CO)] ⁻ (1)	1.992 (7)	2.006 (4)	1.782 (4)	tw ^a
[Fe(TpivPP)(NO ₂)(CO)] ⁻ (2)	1.997 (6)	2.009 (4)	1.789 (5)	tw
[Fe(TpivPP)(NO ₂)] ⁻	1.970 (4)	1.849 (6)		20,22
[Fe(TpivPP)(NO ₂)(PMS)] ⁻	1.990 (6)	1.937 (3)	2.380 (2)	22
[Fe(TpivPP)(NO ₂)(Py)] ⁻	1.990 (15)	1.951 (5)	2.032 (5)	22
[Fe(TpivPP)(NO ₂)(NO)] ^{-b}	1.988 (6)	2.086 (8)	1.792 (8)	21
[Fe(TpivPP)(NO ₂)(NO)] ^{-c}	1.986 (6)	2.060 (7)	1.840 (6)	21
Iron(III) Complex				
[Fe(TpivPP)(NO ₂)(HIm)]	1.974 (2)	1.949 (10)	2.037 (10)	24
[Fe(TpivPP)(NO ₂)(Py)]	1.985 (3)	1.960 (5)	2.093 (5)	24
[Fe(TpivPP)(NO ₂) ₂] ⁻	1.992 (1)	1.970 (5)	2.001 (6)	23
[Fe(TpivPP)(NO ₂)(SC ₆ HF ₅)] ⁻	1.980 (7)	1.990 (7)	2.277 (2)	25
[Fe(TpivPP)(NO ₂)(NO)] ^d	2.000 (5)	2.002 (2)	1.668 (2)	26
[Fe(TpivPP)(NO ₂)(NO)] ^e	1.996 (4)	1.998 (2)	1.671 (2)	26

^aThis work.

^b \perp form.

^c \parallel form.

^dC_{2/c} form.

^eP₂1/n form.

Table 4
Bond Parameters for (Carbonmonoxy)iron Porphyrin Derivatives

Complex	Fe–N _p ^a	Fe–C(CO) ^a	Fe–L ^a	Fe–C–O ^b	C–O ^a	ref.
[Fe(TpivPP)(NO ₂) (CO)] ⁻ (1)	1.992 (7)	1.782 (4)	2.006 (4)	175.5 (4)	1.150 (5)	tw ^c
[Fe(TpivPP)(NO ₂) (CO)] ⁻ (2)	1.997 (6)	1.789 (5)	2.009 (4)	177.5 (4)	1.140 (5)	tw
[Fe(TPP)(Py)(CO)]	2.02 (3)	1.77 (2)	2.10 (1)	179 (2)	1.12 (2)	10
[Fe(Deut)(THF)(CO)]	1.98 (3)	1.706 (5)	2.127 (4)	178.3 (14)	1.144 (5)	13
[Fe(TPP)(SEt)(CO)]	1.993 (4)	1.78 (1)	2.352 (2)	NR	1.17 (1)	14
[Fe(TPP)(1-MeIm)(CO)]	1.999 (7)	1.756 (2)	2.059 (1)	178.91 (17)	1.147 (2)	d
	2.003 (5)	1.793 (3)	2.071 (2)	179.3 (3)	1.061 (3)	11
[Fe(OEP)(1-MeIm) (CO)]	2.000 (3)	1.744 (5)	2.077 (3)	175.1 (4)	1.158 (5)	12
[Fe(TP ₂ Piv ₂ C ₁₂ P)(1- MeIm)(CO)]	1.999 (3)	1.728 (6)	2.062 (5)	~180	1.149 (6)	15
[Fe(β -PocpivP)(1,2- Me ₂ Im)(CO)]	1.973 (8)	1.768 (7)	2.079 (5)	172.5 (6)	1.148 (7)	16
[Fe(C ₂ -Cap)(1-MeIm) (CO)]	1.990 (7)	1.742 (7)	2.043 (6)	172.9 (6)	1.161 (8)	17
	1.988 (13)	1.748 (7)	2.041 (5)	175.9 (6)	1.158 (8)	17
[Fe(OC ₃ OPor)(1-MeIm) (CO)]	1.996 (12)	1.748 (7)	2.027 (5)	173.9 (9)	1.171 (8)	18
[Fe(OC ₃ OPor)(1,2- Me ₂ Im)(CO)]	2.00 (2)	1.713 (8)	2.102 (6)	180 ^e	1.161 (10)	18
[Fe(C ₃ -Cap)(1-MeIm) (CO)]	1.99 (2)	1.800 (13)	2.046 (10)	178.0 (13)	1.107 (13)	19

^aValue in Å^bValue in degrees.^cThis work.^dAn, J.; Beatty, A.; Scheidt, W. R., unpublished result.^eRequired by symmetry.

Table 5Solid-State Mössbauer Parameters for $[\text{Fe}(\text{TpiVPP})(\text{NO}_2)(\text{CO})]^-$ and Related Complexes

	ΔE_Q , mm/s	δ_{Fe} , mm/s	T, K	ref
$[\text{Fe}(\text{TpiVPP})(\text{NO}_2)(\text{CO})]^-$	0.32 0.28	0.18 0.28	293 15	tw ^a tw
Iron(II) Complexes				
$[\text{Fe}(\text{TMP})(\text{Py})_2]$	1.24	0.45	4.2	58
$[\text{Fe}(\text{TPP})(\text{Py})_2]$	1.15	0.40	77	59
$[\text{Fe}(\text{OEP})(\text{Py})_2]$	1.13	0.46	4.2	60
$[\text{Fe}(\text{TPP})(1\text{-VimIm})_2]$	1.00	0.43	4.2	41
$[\text{Fe}(\text{TPP})(\text{Pip})_2]$	1.44	0.51	4.2	61
$[\text{Fe}(\text{TpiVPP})(1\text{-MeIm})_2]$	1.02	0.46	4.2	61
$[\text{Fe}(\text{TMP})(1\text{-MeIm})_2]^b$	1.11	0.45	77	62
$[\text{Fe}(\text{OEP})(1\text{-MeIm})_2]^b$	0.96	0.46	77	62
$[\text{Fe}(\text{TMP})(\text{PMe}_3)(1\text{-MeIm})]^b$	0.75	0.38	77	62
$[\text{Fe}(\text{TMP})(\text{PMe}_3)_2]^b$	0.47	0.36	77	62
$[\text{Fe}(\text{OEP})(\text{PMe}_3)_2]^b$	0.35	0.36	77	62
Iron(II) CO and CS Complexes				
$[\text{Fe}(\text{TPP})(1\text{-MeIm})(\text{CO})]$	0.35	0.20	293	63
$[\text{Fe}(\text{TPP})(\text{Py})(\text{CO})]$	0.57	0.28	293	63
$[\text{Fe}(\text{Tp-OCH}_3\text{PP})(\text{Py})(\text{CO})]$	0.49	0.19	298	64
$[\text{Fe}(\text{Tp-OCH}_3\text{PP})(\text{HIm})(\text{CO})]$	0.36	0.18	298	64
$[\text{Fe}(\text{TpiVPP})(1\text{-MeIm})(\text{CO})]$	0.27	0.27	4.2	30
MbCO	0.35	0.27	4.2	65
$[\text{Fe}(\text{OEP})(4\text{-CNPy})(\text{CS})]$	0.80	0.19	4.2	66
$[\text{Fe}(\text{OEP})(\text{Py})(\text{CS})]$	0.57	0.15	4.2	66
$[\text{Fe}(\text{OEP})(\text{Pip})(\text{CS})]$	0.65	0.19	4.2	66
$[\text{Fe}(\text{OEP})(4\text{-NMe}_2\text{Py})(\text{CS})]$	0.44	0.19	4.2	66
$[\text{Fe}(\text{OEP})(1\text{-MeIm})(\text{CS})]$	0.42	0.14	4.2	66
Iron(II) Nitro Complexes				
$[\text{Fe}(\text{TpiVPP})(\text{NO}_2)]^-$	2.28	0.41	4.2	22
$[\text{Fe}(\text{TpiVPP})(\text{NO}_2)(\text{PMS})]^-$	1.18	0.42	4.2	22
$[\text{Fe}(\text{TpiVPP})(\text{NO}_2)(\text{Py})]^-$	0.93	0.41	4.2	22
{FeNO} ⁷ Complexes				
$[\text{Fe}(\text{TpiVPP})(\text{NO}_2)(\text{NO})]^{-c}$	1.78	0.22	200	21
$[\text{Fe}(\text{TpiVPP})(\text{NO}_2)(\text{NO})]^{-d}$	1.20	0.35	4.2	21
$[\text{Fe}(\text{TPP})(\text{NO})]$	1.24	0.35	4.2	21
$[\text{Fe}(\text{OEP})(\text{NO})]$	1.26	0.35	100	67
$[\text{Fe}(\text{Deut})(\text{NO})]$	1.47	0.39	4.2	68
$[\text{Fe}(\text{TPP})(1\text{-MeIm})(\text{NO})]$	0.73	0.35	4.2	40
$[\text{Fe}(\text{TPP})(4\text{-MePip})(\text{NO})]$	0.91	0.37	4.2	40
Iron(III) Nitro Complexes				
$[\text{Fe}(\text{TpiVPP})(\text{NO}_2)_2]^-$	2.1	0.25	4.2	24
$[\text{Fe}(\text{TpiVPP})(\text{NO}_2)(\text{Py})]^-$	2.2	0.26	4.2	24
$[\text{Fe}(\text{TpiVPP})(\text{NO}_2)(\text{SC}_6\text{HF}_4)]^-$	2.12 2.30	0.22 0.28	293 4.2	25 25
{FeNO} ⁶ Complexes				
$[\text{Fe}(\text{OEP})(\text{Iz})(\text{NO})]^+$	1.99 1.92	-0.07 0.02	293 4.2	69 69
$[\text{Fe}(\text{OEP})(2\text{-MeHIm})(\text{NO})]^+$	1.88	0.05	4.2	70
$[\text{Fe}(\text{OEP})(1\text{-MeIm})(\text{NO})]^{+b}$	1.64	0.02	4.2	71
$[\text{Fe}(\text{OEP})(\text{NO})]\text{ClO}_4$	1.55 1.64	0.13 0.20	293 4.2	69 69
$[\text{Fe}(\text{Tp-OCH}_3\text{PP})(\text{NO}_2)(\text{NO})]$	1.43	0.04	293	26
$[\text{Fe}(\text{TpiVPP})(\text{NO}_2)(\text{NO})]$	1.48 1.43	0.01 0.09	293 4.2	26 26
$[\text{Fe}(\text{TPP})(\text{NO}_2)(\text{NO})]$	1.37 1.36 1.36	0.02 0.13 0.13	293 4.2 77	26 26 72
$[\text{Fe}(\text{OEP})(\text{C}_6\text{H}_4\text{-}p\text{-F})(\text{NO})]$	0.56 0.57	0.05 0.14	293 4.2	73 73

^aThis work.

^bIn dimethylacetamide solution.

^cform.

^d_{||} form.